Nuclear Engineering and Design 386 (2022) 111581

Contents lists available at ScienceDirect

Nuclear Engineering and Design

journal homepage: www.elsevier.com/locate/nucengdes

Extension and application of the TRANSURANUS code to the normal operating conditions of the MYRRHA reactor

A. Magni [a], T. Barani [a,†], F. Belloni [b], B. Boer [b], E. Guizzardi [a], D. Pizzocri [a], A. Schubert [c], P. Van Uffelen [c], L. Luzzi [a,*]

[a] Politecnico di Milano, Department of Energy, Nuclear Engineering Division, via La Masa 34, 20156 Milano, Italy
[b] Studiecentrum voor Kernenergie (SCK CEN), Boeretang 200, 2400 Mol, Belgium
[c] European Commission, Joint Research Centre, Karlsruhe, Germany

ARTICLE INFO

Keywords:
Generation IV
MYRRHA reactor
Cladding creep and swelling
Fuel performance code
TRANSURANUS

ABSTRACT

This work deals with the performance analysis of the MYRRHA hottest fuel pin in normal operating conditions, employing the TRANSURANUS fuel performance code, with the aim of assessing the current design specifications considering conservative design limits. To allow the proper simulation of the MYRRHA pin behaviour, TRANSURANUS is extended with novel correlations for the creep and void swelling response of the specific cladding material (DIN 1.4970). The analysis of the best-estimate *reference* scenario is complemented by a sensitivity analysis on models describing fuel and cladding phenomena and properties, determining those which most affect the pin performance results and identifying the *worst-case* scenarios. The simulation outcomes point out the high level of safety related to the MYRRHA fuel pin performance in normal operating conditions, which keeps far from any design or critical limit, even in the most challenging (*worst-case*) scenarios.

1. Introduction

The need for safe and sustainable technologies has strongly affected the nuclear energy field in the recent decades, leading to the foundation of the Generation IV International Forum (GIF), aimed at introducing a new generation of nuclear reactors (GIF (Generation IV International Forum), 2014). In this context, the European Sustainable Nuclear Industrial Initiative (ESNII) program was launched in 2010 to foster the development of four fast neutron spectrum facilities and demonstrators (ESNII, 2010): ASTRID as sodium fast reactor (SFR) (Beck et al., 2017), ALFRED as lead fast reactor (LFR) (Grasso et al., 2014), MYRRHA (Multi-purpose Hybrid Research Reactor for High-tech Applications) as lead–bismuth eutectic (LBE)-cooled fast reactor (Aït Abderrahim et al., 2019), ALLEGRO as gas fast reactor (GFR) (Stainsby et al., 2011; Pónya and Czifrus, 2017). The MYRRHA facility under development at SCK CEN has gained an important role in the development path leading to an Accelerator-Driven System (ADS), considering the recent growing interest in ultimate radioactive waste management, proliferation resistance and sustainability improvement by better use of fuel resources (Aït Abderrahim et al., 2020). MYRRHA aims to demonstrate the accelerator-driven system concept and to operate as a flexible Generation IV irradiation facility for R&D purposes.

Assessing the thermal–mechanical behaviour of fuel pins for Generation IV fast reactor systems is a key point during reactor design, due to the extremely demanding operating conditions (high temperatures, extended fast neutron irradiation, chemically aggressive coolant environment) (Pioro, 2016). Fuel performance codes are typically used for this purpose (Van Uffelen and Suzuki, 2012), allowing to account for the interrelationship among the numerous phenomena affecting the fuel pin under irradiation (Guerin, 2012; Waltar et al., 2012). Improving the predictive capabilities of fuel performance codes related to materials and operating conditions envisaged for Generation IV fast reactors, towards their safety assessment, is one of the objectives of the INSPYRE (Investigations Supporting MOX Fuel Licensing in ESNII Prototype Reactors) H2020 European Project (EERA-JPNM, 2017).

In line with the ESNII roadmap, the work presented in this paper deals with the preliminary pin performance assessment of the MYRRHA reactor. In particular, the present work refers to the MYRRHA design "Revision 1.6 configuration" (De Bruyn et al., 2016; Luzzi et al., 2019), defined after earlier design proposals and analyses performed in (Aït

* Corresponding author.
E-mail address: lelio.luzzi@polimi.it (L. Luzzi).
† Current address: CEA, DES/IRESNE/DEC/SESC/LSC, Cadarache center, 13108 Saint-Paul-Les-Durance, France.

https://doi.org/10.1016/j.nucengdes.2021.111581
Received 22 July 2021; Received in revised form 10 November 2021; Accepted 20 November 2021
Available online 9 December 2021

Abderrahim et al., 2012; De Bruyn et al., 2015; Engelen et al., 2015; Aït Abderrahim et al., 2005). At SCK CEN the in-house fuel performance code MACROS has previously been applied for the simulation and design of the MYRRHA fuel pin (Lemehov et al., 2003; Lemehov et al., 2005; Boer et al., 2012).

In this paper, modelling extensions of the TRANSURANUS fuel performance code (European Commission, 2020; Lassmann, 1978) towards the specific cladding material employed for the MYRRHA pins and the application of TRANSURANUS to the MYRRHA normal operating conditions, performed at Politecnico di Milano, are described. The TRANSURANUS code (version v1m1j20) improvements concern the creep and void swelling properties of the DIN 1.4970 austenitic stainless-steel cladding material (De Bruyn et al., 2016). The current modelling of cladding thermal and mechanical properties in the TRANSURANUS fuel performance code mainly concerns a generalized version of the 15-15Ti stainless steel, with some specific correlations for AIM1 and D9 (European Commission, 2020). These capabilities have been reviewed at Politecnico di Milano as part of a LFR-oriented version of TRANSURANUS, conceived to analyse the pin performance and provide safety indications about the ALFRED lead-cooled reactor (Luzzi et al., 2014). Properties for lead and lead–bismuth eutectic (LBE) as liquid metal coolants have also been comprehensively reviewed and implemented in TRANSURANUS by (Agosti et al., 2013), based on (OECD/NEA, 2007). The performance analysis of a fuel pin in LBE coolant environment, focusing on the behaviour of different cladding materials, has been preliminarily investigated in (Agosti et al., 2011). The improvement path followed in recent years to extend the applicability of the TRANSURANUS code to fast reactor conditions included also models of fuel material properties, in particular for U-Pu mixed-oxides (MOX) eventually containing minor actinides for transmutation purposes (Di Marcello et al., 2012; Bouineau et al., 2013; Di Marcello et al., 2014).

In this work, specific models describing the creep (both thermal and irradiation-induced) and swelling behaviour of the DIN 1.4970 cladding material have been integrated in the TRANSURANUS code, including both models existing in the open literature and original ones developed by fitting available experimental data. The focus is on these cladding properties since the cladding represents the first safety barrier for the reactor operation and its integrity is of concern, especially in fast reactor irradiation conditions (i.e., high fluxes of high-energy neutrons). Thermal and irradiation creep affect the cladding geometry and the fuel-cladding gap dynamics, reflecting on the fuel temperature regime and cladding mechanical loads (accounting for contact pressure and stress relaxation by creep in case of gap closure) (Guerin, 2012; Waltar et al., 2012). Void swelling impacts as well on the cladding geometry and on the coolant channel, influencing the pin coolability (Pitner et al., 1995).

The extended version of the TRANSURANUS code has been adopted for the analysis of the MYRRHA fuel and cladding performance under normal operating conditions. Design limits for the MYRRHA pin originating from either a physical phenomenon (i.e., fuel melting) or generally accepted as engineering principles (limits on stresses and strains) are herein assumed. *Reference-case* and *worst-case* scenarios, both concerning the hottest pin condition to draw conservative evaluations, are herein identified and analysed. The *reference case* is defined by simulating the fuel and cladding behaviour through the recommended (in the standard code version) set of models suitable for the MYRRHA pin materials and irradiation conditions. The *worst cases* instead, in terms of peak fuel temperature and cladding strain, result from a model sensitivity analysis and aim at investigating the impact of modelling uncertainties for key phenomena and properties relevant in the reference scenario. This allows verifying the compliance with the considered design limits also in the case of the worst pin performance predicted by the TRANSURANUS code.

The structure of the paper is as follows. A general description of the MYRRHA reactor core is briefly provided in Section 2, along with the details of the specific case study herein analysed. In Section 3, the dedicated modelling of the MYRRHA cladding material is presented, as essential step towards the performance analysis of the MYRRHA hottest fuel pin by means of the TRANSURANUS code, which is shown and discussed in Section 4. Finally, conclusions are drawn in Section 5.

2. MYRRHA reactor configuration and case study description

MYRRHA "Revision 1.6" (De Bruyn et al., 2016; Van Tichelen et al., 2020) is a 100 MW_{th} pool-type reactor, with an operating power of 70 MW_{th} in subcritical mode. It is an accelerator-driven system (ADS), featured by an accelerated proton energy of 600 MeV and a beam current of 1.74 mA. It employs lead–bismuth eutectic (LBE) as a coolant and as moving spallation target, while the secondary coolant is saturated water / steam, with an inlet (at the steam generator) temperature of 200°C (De Bruyn et al., 2015; Van Den Eynde et al., 2015). The pool configuration foresees an internal diaphragm dividing the hot (upper) plenum from the cold (lower) one, in communication through two axial pumps and two primary heat exchangers per pump.

The reactor core in subcritical configuration houses a central spallation target, a maximum of 6 in-pile test sections (IPS) for irradiation purposes, 72 wrapped fuel assemblies, and other dummy or lateral reflector/shielding elements (Aït Abderrahim et al., 2019). The fuel assemblies are constituted by a hexagonal bundle of 127 cylindrical fuel pins wounded by a spiral wire to obtain a tight triangular arrangement (Van Tichelen et al., 2020). Each fuel pin is composed of a stack of uranium–plutonium mixed-oxide (MOX) pellets, with 5% as-fabricated porosity, hosted by a support tube in the lower plenum and by a spring in the upper one. The fuel is 30% enriched in plutonium, whereas uranium has the natural isotopic composition (Luzzi et al., 2019). The selected cladding material is DIN 1.4970, an austenitic stainless-steel of the double stabilized 15-15Ti family (cold-worked at 15–20%) (Luzzi et al., 2019). Its composition ranges, reported in Table 1, feature trace constituents and a Ti content around 0.5 wt.%, while the 15 wt.% content of the major alloying elements (Ni and Cr) provides the bulk of its thermo-mechanical properties, common to all the steels pertaining to the 15-15Ti family (Luzzi et al., 2014).

The operating schedule of MYRRHA consists of irradiation cycles: each fuel assembly spends about 90 days inside a specific batch of the core before 30 days reactor stop with reshuffling (Van Den Eynde et al., 2015), accumulating in total more than 1000 days under irradiation and reaching a lifetime of 5 years. Twelve batches representative for the fuel handling strategy were identified, as shown in Fig. 1 (Van Den Eynde et al., 2015).

The present analysis of the MYRRHA fuel pin performance focuses on a *hypothetical hottest pin*, identified on purpose to draw conservative conclusions. The position of the real hottest pin in a MYRRHA fuel

Table 1
Chemical composition of the DIN 1.4970 alloy (Cautaerts et al., 2017).

Element	Content (wt.%)
B	0.0030–0.0080
C	0.080–0.120
Ca	<0.010
Co	<0.030
Cr	14.5–15.5
Cu	<0.050
Fe	~66.0
Mn	<2.0
Mo	1.0–1.4
N	<0.015
Ni	14.5–15.5
P	<0.015
S	<0.015
Si	0.3–0.6
Ti	0.3–0.55
Ta	<0.02
V	<0.05

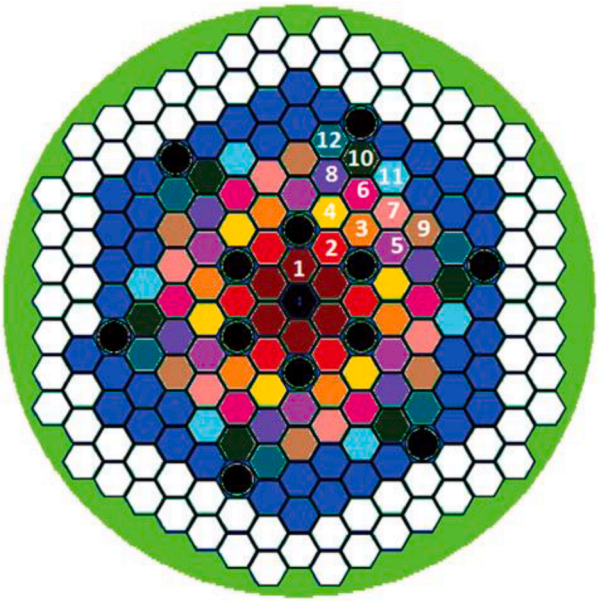

Fig. 1. Batch positions in the MYRRHA core (Van Den Eynde et al., 2015).

assembly changes between one batch and the following, moving from an inner-core position at beginning of life to average or colder ones. In this work, it is assumed that the same fuel pin is located in the hottest pin position during every batch. This assumption results in a fuel pin sustaining an overestimated load (in terms of neutron flux and temperature) throughout the irradiation history[1], which is shown in Fig. 2a. Both linear power and fast neutron flux (referring here to neutrons with energy above the threshold of 1 MeV) significantly decrease in time moving towards outer batches (i.e., from batch 1, beginning of life, to batch 12, end of life), while they are kept constant within a batch. In parallel, the power and neutron flux axial profiles (Fig. 2b) show a flattening with fuel burn-up (Luzzi et al., 2019). The peak linear power (at batch 1, at the fuel column mid-plane) is about 230 W cm^{-1}, while the corresponding peak fast neutron flux is about $1.6 \cdot 10^{15}$ cm^{-2} s^{-1}.

Concerning the coolant conditions, constant inlet temperature and pressure have been considered, equal to 245°C and 0.6 MPa, respectively (Luzzi et al., 2019). According to the hottest pin hypothesis, conversely, the coolant mass flow rate changes during irradiation depending on the sub-channel the hottest pin belongs to during each batch. The coolant mass flow rate is 0.48 kg s^{-1} for the inner hottest pin (i.e., located in an inner position of a fuel assembly), 0.56 kg s^{-1} for the intermediate positions, while 0.76 kg s^{-1} for the peripheral channels of the assembly.

In order to assess the MYRRHA fuel pin performance according to the current specifications and assumptions for the design version "1.6" of the reactor, design limits have been considered and the corresponding safety margins evaluated. The safety limits considered in this work for the MYRRHA fuel pin are conservative, to verify the fuel pin integrity by demonstrating the absence of pin failures from both the fuel and the cladding points of view. Corresponding to this main requirement, design limits are defined in Table 2, regarding:

1. The peak fuel temperature, limited to avoid the occurrence of fuel melting.
2. The cladding mechanical behaviour, in terms of maximum allowable stresses and strains, to prevent cladding fracture.

[1] In the following, the *hypothetical hottest pin* herein considered will be simply referred to as "hottest pin", different from the actual hottest pin of the single batches (i.e., experiencing the worst irradiation conditions during each batch).

The fuel temperature limit is derived from the melting (solidus) temperature of the MYRRHA fuel (accounting for its composition and target burn-up), according to data and correlations available in the open literature (Kato et al., 2008; Yamamoto et al., 1993; Aitken and Evans, 1968; Lyon and Baily, 1967; Magni et al., 2020). Hence, taking into account the initial deviation from stoichiometry of the MYRRHA fuel (x = 2 – O/M = 0.03) and a conservative upper limit on the fuel burn-up of 10% FIMA, the following fuel temperature limit (encompassing the trend of the experimental data within a 2σ deviation) is conservatively set:

$$T_{fuel} \leq 2870 \text{ K } (2597^{\circ}\text{C}) \quad (1)$$

For what concerns the cladding behaviour, it is known that above a temperature of ~ 350°C the LBE corrosion effects on the cladding outer surface can potentially degrade the austenitic stainless-steel material, depending on the conditions (e.g., type of flow, oxygen content in the LBE) (Klok, 2018). These effects are typically more severe with increasing temperature and therefore the exposure of the cladding at elevated temperatures must be avoided. A well-established design limit is not currently available given the still ongoing research on the complex corrosion effects. Instead, a limit temperature for the cladding inner surface is adopted (500°C), which should result in a negligible fuel-side corrosion (Bradbury et al., 1978).

3. Extension of the TRANSURANUS code for the MYRRHA fuel pin simulation

The TRANSURANUS fuel performance code (European Commission, 2020; Lassmann, 1978) is widely assessed and validated for light water reactor applications (Lassmann, 1992; Van Uffelen et al., 2008; Pastore et al., 2009). Its adoption to study innovative systems of Generation IV calls for code improvements to deal with different working conditions and specific materials. Development efforts have already been spent to extend TRANSURANUS to fast reactor irradiation conditions and materials, targeting in particular fuels for Gen-IV applications. Recent modelling advancements concerned the redistribution of plutonium and americium in MOX and minor actinide-bearing MOX, for both lead- and sodium-cooled fast reactor irradiation conditions (Di Marcello et al., 2012; Di Marcello et al., 2014). These activities allowed the proper performance analysis of fuel pins for fast and liquid–metal Generation-IV reactors, see e.g., (Luzzi et al., 2014; Bouineau et al., 2013). The latest upgrades of the TRANSURANUS code concerned the modelling of thermal conductivity and melting temperature of mixed-oxide fuels (Magni et al., 2020; Magni et al., 2021), the evolution of actinide concentrations and helium production with burn-up (Cechet et al., 2021), and the mechanistic modelling of fission gas behaviour (also in restructured fuel regions, i.e., in columnar grains and in the high burn-up structure) embedded in the SCIANTIX grain-scale code (Pizzocri et al., 2020), coupled with TRANSURANUS.

In this Section, a dedicated modelling of the specific MYRRHA cladding material (DIN1.4970), extending the TRANSURANUS code predictive capabilities and being a crucial step towards the fuel pin performance analysis performed in Section 4, is presented.

Novel correlations for the creep and swelling behaviour (both thermal and irradiation-induced) of DIN 1.4970 have been developed and implemented in TRANSURANUS. Specifically, original correlations for the thermal and irradiation creep strain rates and for the thermal creep time-to-rupture have been developed by fitting experimental data available in literature. Moreover, existing correlations for the void swelling rate of DIN 1.4970 have been introduced in the code (Lemehov et al., 2011). Instead, the correlations already embedded in the code for the main thermo-mechanical properties (e.g., thermal conductivity, elasticity constants, density, specific heat, melting temperature) of generic 15-15Ti steels are at this stage deemed reliable also for DIN 1.4970 (European Commission, 2020). In the following sub-sections, the

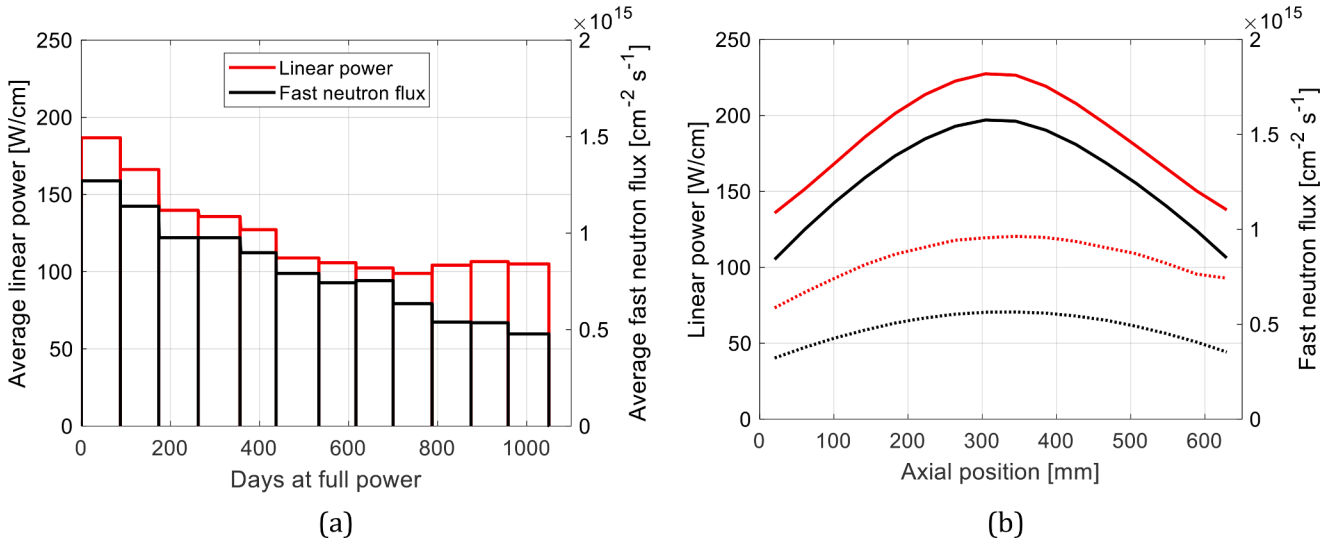

Fig. 2. Linear heat rate (red curves) and fast neutron flux (black curves) of the MYRRHA hottest pin: (a) axially average irradiation history in normal operating conditions and (b) axial profiles at batch 1 (solid line) and at batch 12 (dotted line).

Table 2
Conservative design limits adopted to assess the MYRRHA fuel pin design in normal operating conditions.

Quantity	Adopted design limit	References
Peak fuel temperature	< 2597°C	(Kato et al., 2008; Yamamoto et al., 1993; Aitken and Evans, 1968; Lyon and Baily, 1967; Magni et al., 2020)
Peak cladding inner surface temperature during normal operation (fuel-side corrosion)	< 500°C	(Bradbury et al., 1978)
Cladding stress during normal operation	$\sigma \leq \frac{2}{3}\sigma_{0.2}$ [a]	(Holmstrom et al., 2017; Strafella et al., 2017a,b)
Cladding plastic strain (ε_L^P)	0.5%	(Luzzi et al., 2019)
Cladding CDF [b]	$\sum_{\Delta t}\left\{\frac{\Delta\varepsilon^P}{\varepsilon_L^P}+\frac{\Delta t}{t_R(t)}\right\}_{t\to t+\Delta t} \leq 1$ (rupture at $\varepsilon_L^P = 0.5\%$)	(Waltar et al., 2012)

[a] $\sigma_{0.2}$ is defined as the stress at which 0.2% plastic deformation of the material occurs.

[b] The Cumulative Damage Function (CDF) approach allows predicting the cladding failure by considering the accumulation of damage fractions from both normal and transient operating conditions. The steady-state component, herein considered, is computed as the ratio between a time-increment (Δt) and the time-to-rupture (t_R), added to the ratio between the accumulation of plastic strain increments $\Delta\varepsilon^P$ and the plastic rupture strain ε_L^P associated to the conditions existing at that time step itself (Waltar et al., 2012). The plastic contribution to the CDF does not include the radiation-induced creep or swelling components.

novel correlations herein developed or selected for implementation in TRANSURANUS are presented and shown, indicating for each property the MYRRHA cladding operative range (Figs. 3 – 6).

3.1. Thermal and irradiation creep strain rate

The current uncertainty on the creep experimental data on 15–15 steels is relevant: up to two orders of magnitude, as shown by Fig. 3 for the thermal creep. Furthermore, given the scarcity of data in the temperature range relevant for the MYRRHA cladding (270°C – 450°C) (Cautaerts et al., 2017), the extrapolation of the available correlations beyond their original validity range (i.e., towards lower temperatures and low stress levels) is sometimes applied. The incorporation in fuel performance codes of an updated and specific thermal creep correlation is also relevant in the perspective of future analyses of pin performance under off-normal conditions, since at the nominal temperatures of the MYRRHA cladding the expected thermal creep is null or limited.

The state-of-the-art TRANSURANUS code includes the modelling of the thermal creep of DIN 1.4970 according to a correlation developed by Többe (Többe, 1975), involving a Nabarro-Herring formulation:

$$\dot{\varepsilon}_{th} = C_1 \cdot \exp\left(-\frac{C_2}{T}\right) \cdot \sinh\left(\frac{C_3\sigma_{eq}}{T}\right) \quad (2)$$

where $\dot{\varepsilon}_{th}$ (h^{-1}) is the Von Mises equivalent thermal creep strain rate, T (K) is the absolute temperature, σ_{eq} (MPa) the Von Mises equivalent stress, and C_1, C_2, C_3 are model parameters (Többe, 1975). The same functional form is also reported by (Lassmann and Moreno, 1977), apart from the missing temperature-dependence in the hyperbolic sine factor.

A novel correlation has been developed based on recent results of creep tests performed by the DeBeNe consortium on annealed and cold-worked 15–25% DIN 1.4970 (Cautaerts et al., 2017), referring to the temperature range 600–750°C. In (Cautaerts et al., 2017), a correlation tailored only on the non-aged specimen data was elaborated, exploiting an Arrhenius temperature dependence (i.e., exponential on the temperature). The original correlation herein proposed also features the Arrhenius functional form, but fitting the activation energy and two model parameters on the whole DeBeNe dataset in order to consider both aged and non-aged specimens:

$$\dot{\varepsilon}_{th} = \left(\sinh\left(0.0123\sigma_{eq}\right)\right)^{2.332} \cdot \exp\left(-\frac{1.205\cdot 10^5}{R\cdot T}\right) \quad (3)$$

where the equivalent thermal creep strain rate $\dot{\varepsilon}_{th}$ is provided in h^{-1} and R is the gas constant (~8.314 J mol^{-1} K^{-1}). The novel model is plotted in Fig. 3 together with the standard Többe's correlation (Eq. (2), (Többe, 1975)) and the experimental raw data (Cautaerts et al., 2017), showing very good predictions at temperatures up to 700°C, whereas the Többe's correlation (Többe, 1975) proves to be more reliable as temperature exceeds 700°C. For the purpose of the performance analysis of MYRRHA fuel pins, both correlations will be adopted to model the cladding creep behaviour (Section 4). Despite the fact that the Többe correlation (Többe, 1975) proves more accurate against the available dataset at higher temperatures (e.g., at 750 °C, as shown in Fig. 3) where thermal creep dominates, the novel correlation supplies more conservative estimations at the MYRRHA cladding working temperatures (i.e., 270°C –

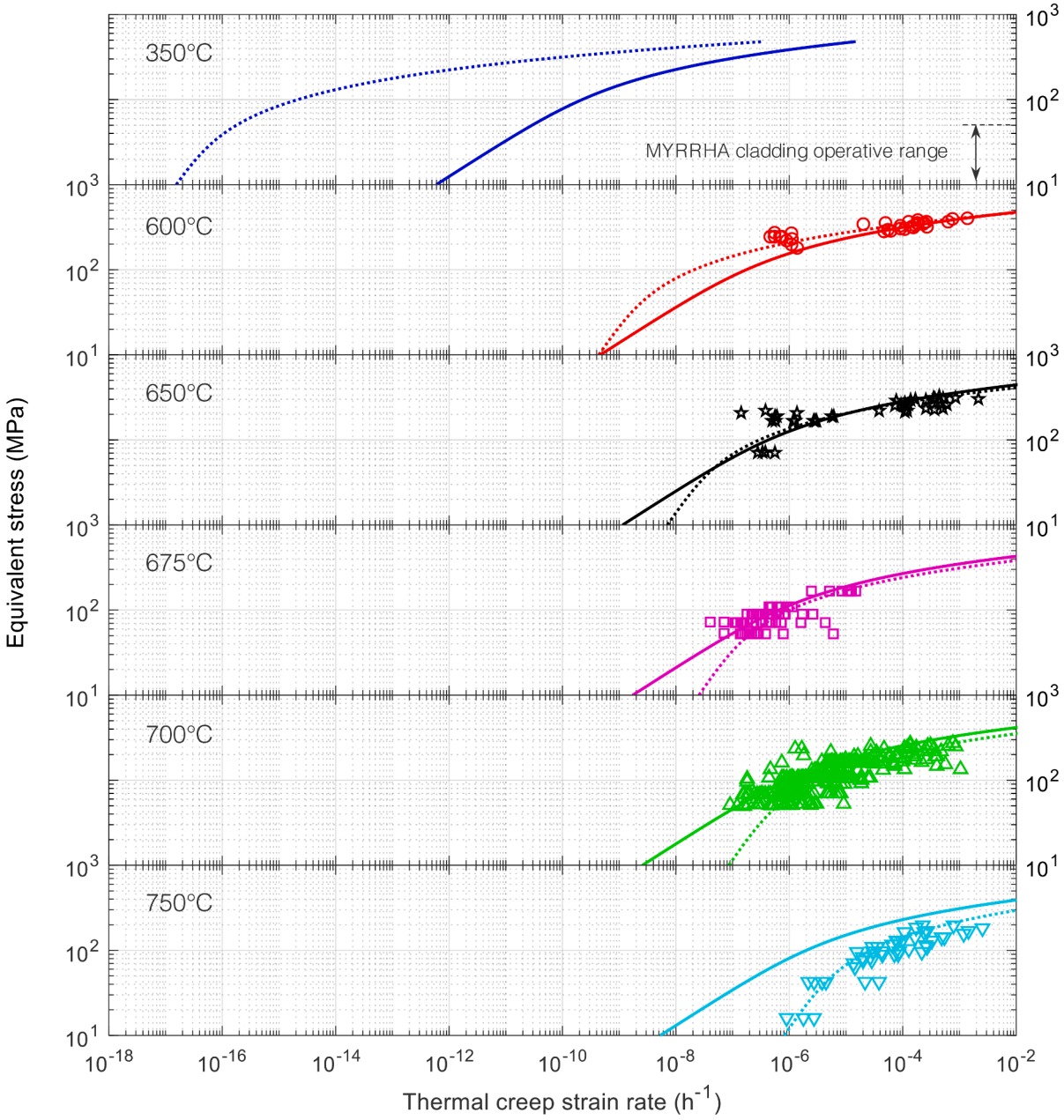

Fig. 3. Thermal creep strain rate predicted by Többe's correlation (Többe, 1975) (Eq. (2), dotted lines) and by the correlation developed in the present work (Eq. (3), solid lines), compared to the available experimental data (Cautaerts et al., 2017). The upper plot corresponds to a representative MYRRHA cladding temperature in normal operating conditions (350°C).

450°C), being representative of a faster thermal creep mechanism at equal equivalent stress.

Concerning the irradiation creep strain rate, which dominates at the MYRRHA cladding working temperatures, the state-of-the-art TRANSURANUS code does not include a model suitable for the specific composition of the DIN 1.4970 alloy. Instead, it is equipped with a generic correlation for 15-15Ti steels developed by Többe (Többe, 1975):

$$\dot{\varepsilon}_{irr} = k \cdot \overline{E} \cdot \sigma_{eq} \cdot \phi \tag{4}$$

where $\dot{\varepsilon}_{irr}$ (h^{-1}) is the Von Mises equivalent irradiation creep strain rate, $\overline{E}$ (MeV) is the mean neutron energy, ϕ (cm^{-2} s^{-1}) the neutron flux, σ_{eq} (MPa) is again the Von Mises equivalent stress and k is a fitting constant. Többe's correlation is similar to one of the models included in the open-literature review by Matthews and Finnis (equation (61) in (Matthews and Finnis, 1988), considered as a simple model valid for steady-state irradiation and expressing the relaxation strain rate of the material within a displacement spike, under an applied load). This model includes the dependence to the effective volume of the spike, which can be considered proportional to the neutron energy (on which the irradiation creep strain rate depends according to Többe's correlation, Eq. (4)).

Few studies of the irradiation creep behaviour of the DIN 1.4970 cladding steel can be found in the open literature. A data-driven approach has been pursued to derive a correlation based on the experimental data reported by (Grossbeck et al., 1990), for a cold-worked and aged DIN 1.4970 tested in the BR-2 reactor at 100 MPa. As suggested in

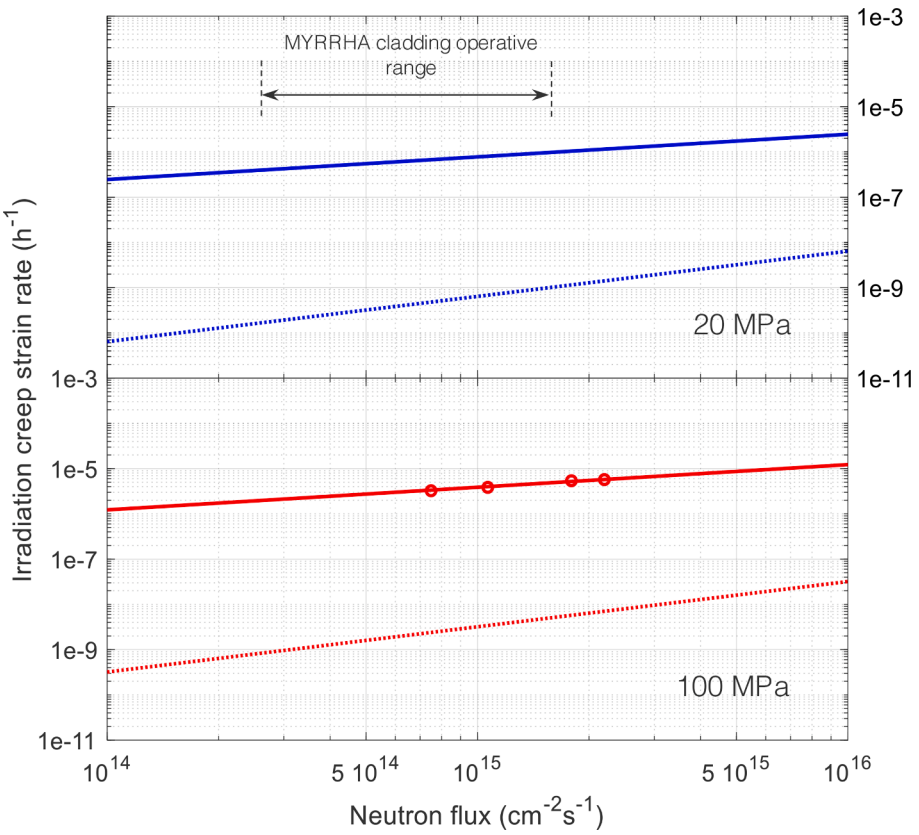

Fig. 4. Irradiation creep strain rate as a function of the fast neutron flux (logarithmic scale), as predicted by Többe's correlation (Többe, 1975) (Eq. (4), dotted lines) and by the correlation developed in the present work (Eq. (5), solid lines), against experimental data ((Grossbeck et al., 1990), red circles). The blue and red curves correspond to different equivalent stresses, i.e., 20 MPa (representative of the MYRRHA cladding condition in normal operation) and 100 MPa, respectively.

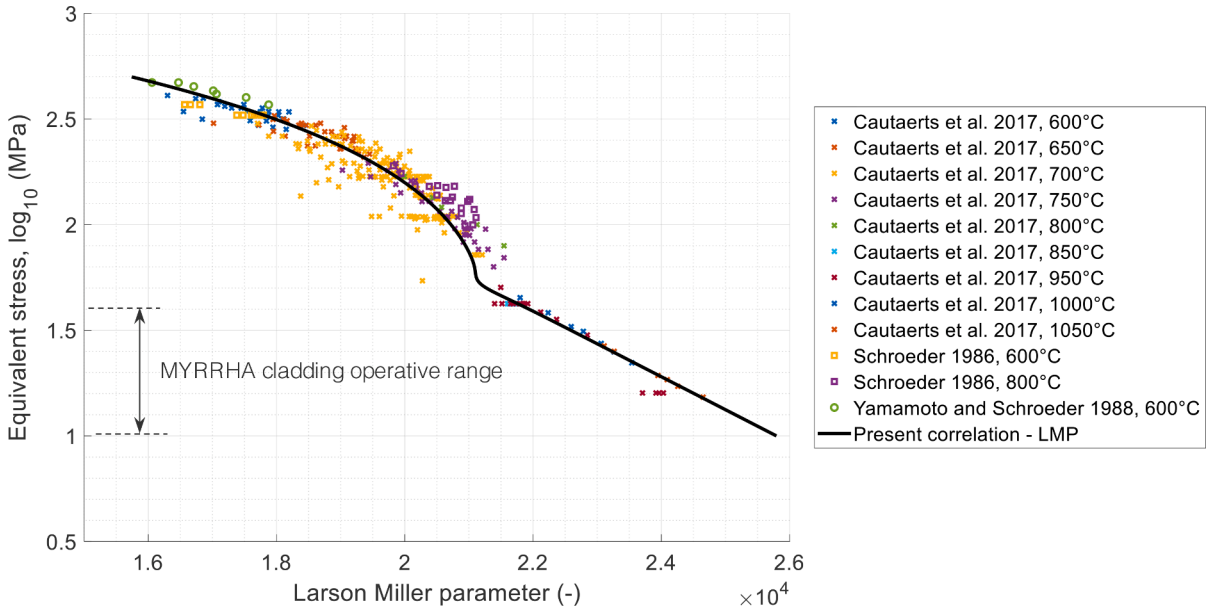

Fig. 5. Comparison between the experimental data for the time-to-rupture of DIN 1.4970 (Cautaerts et al., 2017; Schroeder, 1986; Yamamoto and Schroeder, 1988) and the correlation for the Larson-Miller parameter (LMP) derived in this work (Eqs. (7) and (8)).

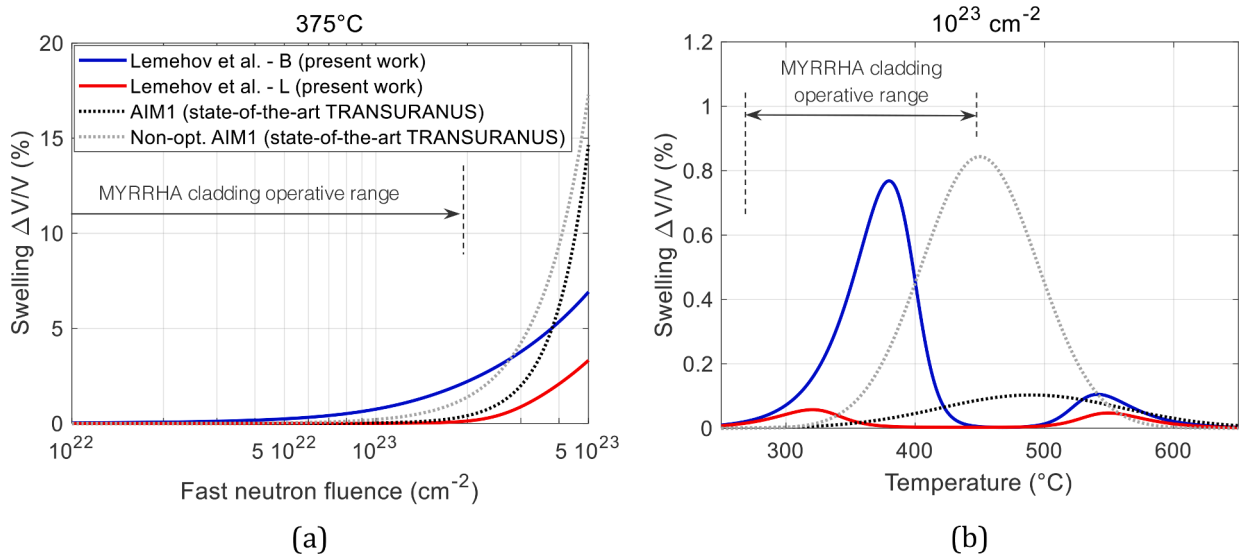

Fig. 6. Comparison between the DIN 1.4970 void swelling models from Lemehov et al. (Eqs. 9–11, (Lemehov et al., 2011)) and the models for AIM1 available in the TRANSURANUS state-of-the-art code (European Commission, 2020; Luzzi et al., 2014): (a) at a fixed temperature representative of the MYRRHA cladding and (b) at a fixed neutron fluence representative of the MYRRHA end-of-life conditions. The Lemehov et al. swelling curves in (a) (blue and red curves) are obtained by summing the swelling increments due to the fluence variations (expressed by Eq. (9)).

(Grossbeck et al., 1990), the irradiation creep strain rate data[2] have been interpolated by means of a square root dependence[3] on the neutron flux (best-fitting the associated data), while keeping the other dependences unchanged with respect to Többe's correlation (Többe, 1975):

$$\dot{\varepsilon}_{irr} = 1.266 \cdot 10^{-15} \cdot \overline{E} \cdot \sigma_{eq} \cdot \sqrt{\phi} \tag{5}$$

In Fig. 4, the novel correlation is plotted against the available experimental points on DIN 1.4970 and compared to Többe's correlation (Többe, 1975). The comparison reveals a difference of up to three orders of magnitude between the two curves, with the standard TRANSURANUS model (Többe, 1975) predicting too low strain rate values compared to the available data. In view of this big discrepancy, it is deemed essential to assess the MYRRHA fuel pin performance by exploiting both models in the context of a sensitivity analysis (Section 4), since very different performance scenarios may arise.

3.2. Thermal creep time-to-rupture

The state-of-the-art version of the TRANSURANUS code is equipped with a creep time-to-rupture correlation accounting for the stress and temperature conditions existing in the cladding and based on the P parameter, a reformulation of the Larson-Miller parameter considered suitable for 15-15Ti cladding steels (European Commission, 2020; Luzzi et al., 2014). The cladding failure by thermal creep can be of concern and has to be monitored under Pellet-Cladding Mechanical Interaction (PCMI) conditions (i.e., closed fuel-cladding gap) (Waltar et al., 2012). It should be underlined that, under normal operating conditions, thermal creep is not expected in the MYRRHA cladding (due to the low operative temperatures, 270°C – 450°C), but the incorporation in fuel performance codes of an advanced modelling is part of a wider development enabling the proper consideration of transient conditions.

The current TRANSURANUS correlation for the time-to-rupture has been compared to available experimental data for annealed and cold-worked DIN 1.4970 (Cautaerts et al., 2017; Schroeder, 1986; Yamamoto and Schroeder, 1988), unveiling rather conservative estimations especially at low stresses. Correspondingly, a new model has been derived, suitable for the MYRRHA pin performance analysis and more accurate in predicting the available experimental data. The Larson-Miller parameter (LMP, defined as in Eq. (6) and broadly used in literature (Luzzi et al., 2014; Larson and Miller, 1952)) has been selected for the new approach:

$$\mathrm{LMP} = \mathrm{T} \cdot (C + \log_{10} t_R) \tag{6}$$

where T (K) is the absolute temperature, t_R (h) is the time-to-rupture and C is a model parameter, equal to 17.6 for the MYRRHA cladding steel under consideration (Cautaerts et al., 2017). The two functional shapes suggested in (Cautaerts et al., 2017) for two stress ranges (i.e., equivalent stress higher/lower than 1.7 MPa, as shown in Fig. 5) have been adopted, while determining the correlation coefficients on the whole datasets from (Cautaerts et al., 2017; Schroeder, 1986; Yamamoto and Schroeder, 1988). In addition, the two curves have been connected through a sigmoidal function ω (Eq. (7)), obtaining the LMP correlation as a function of the equivalent stress reported by Eq. (8):

$$\omega = \frac{1}{2}\left[1 + \tanh\left(\frac{\sigma_{eq} - 52.47}{6.51}\right)\right] \tag{7}$$

$$\begin{aligned} \mathrm{LMP} = {} & \left[-6.41 \cdot 10^3 \cdot \log_{10}\sigma_{eq} + 3.22 \cdot 10^4\right] \cdot \left(1 - \omega(\sigma_{eq})\right) \\ & + \left[\left(\frac{2.64}{21.01} \cdot \left(\log_{10}\sigma_{eq} - 1.21\right) + 1\right) \cdot \right. \\ & \left. \left(22.01 - \exp\left(1.46 \cdot \left(\log_{10}\sigma_{eq} - 1.21\right)\right)\right) \cdot 10^3\right] \cdot \omega(\sigma_{eq}) \end{aligned} \tag{8}$$

where σ_{eq} (MPa) is the Von Mises equivalent stress. In Fig. 5, the derived LMP approach is compared with the entire set of experimental points, showing an excellent capability to follow the data disposition both at high and at low stresses. Reversing Eq. (6), the time-to-rupture can be calculated accordingly. The operative condition range of the MYRRHA cladding, reported in Fig. 5, indicates that a large margin exists before cladding failure by thermal creep.

The Cumulative Damage Function (CDF) is determined by summing over all the simulation time steps the ratio between each time step and

[2] A conversion factor equal to $10^{21}\,\mathrm{dpa}^{-1}\mathrm{cm}^{-2}$ has been assumed to express the experimental data as a function of the neutron flux, considering as reference the typical values valid for thermal and fast reactors suggested in (Lemaignan, 2010).

[3] The linear dependence on the neutron flux, employed by Többe (1975), corresponds to a higher root mean square error over the Grossbeck et al. data (Grossbeck et al., 1990), which are instead best-fitted by a square root function of the neutron flux.

the calculated creep time-to-rupture in the actual conditions, accounting also for the accumulation of plastic strain increments with respect to the actual plastic rupture strain (as specified in Table 2). A CDF value smaller than one indicates that the cladding does not fail because of thermal creep, hence corresponding to the design limit for cladding integrity specified in Table 2.

3.3. Void swelling

In the TRANSURANUS reference code version (v1m1j20), two general correlations modelling the swelling behaviour of 15-15Ti steels are available, referring either to AIM1 or to a non-optimized version of the steel (European Commission, 2020; Luzzi et al., 2014). These correlations consider the swelling rate dependence on the fast neutron fluence (the swelling driving force) and on temperature, while neglecting the contribution of stress and the interaction with creep. Also, they account for a rapid volumetric growth of the cladding material after an incubation period in which no swelling occurs (Guerin, 2012; Waltar et al., 2012).

A specific model for DIN1.4970, employed in the fuel performance code MACROS (Lemehov et al., 2012) and presented in (Lemehov et al., 2011), has been implemented in TRANSURANUS for the MYRRHA pin performance analysis[4,5]:

$$\delta\left(\frac{\Delta V}{V}\right) = \dot{S}_0\left(\delta\Phi + \alpha\cdot\ln\left(\frac{1+\exp\left(\frac{\Phi_0-\Phi-\delta\Phi}{\alpha}\right)}{1+\exp\left(\frac{\Phi_0-\Phi}{\alpha}\right)}\right)\right) \tag{9}$$

where $\delta\left(\frac{\Delta V}{V}\right)$ (%) is the cladding swelling variation due to the fast (E > 0.1 MeV) neutron fluence increment $\delta\Phi$, starting from fluence Φ (both expressed in cm^{-2}). α is a constant equal to $1/(3{\cdot}10^{-23})$ cm^{-2}, while $\dot{S}_0$ (%/cm^{-2}) and Φ_0 (cm^{-2}) are the swelling rate and the incubation fluence, respectively. Two versions of the DIN 1.4970 are herein accounted for: the "B" version corresponds to a standard DIN 1.4970 version, while the "L" is a swelling-strengthened version, featured by a Si content up to 0.96% (Lemehov et al., 2011). Hence, $\dot{S}_0$ and Φ_0 are computed through Eq. (10) for the "B" version of the steel, while through Eq. (11) for the "L" version of DIN 1.4970:

$$\dot{S}_0 = 0.25\cdot\frac{\tanh\left(\frac{T-698}{50}\right)-\tanh\left(\frac{T-718}{50}\right)}{2\tanh\left(\frac{718-698}{100}\right)}\cdot\frac{1}{5{\cdot}10^{21}}$$

$$\Phi_0 = 60\cdot\frac{\tanh\left(\frac{T-698}{50}\right)-\tanh\left(\frac{T-773}{50}\right)}{2\tanh\left(\frac{773-698}{100}\right)}\cdot\left(5{\cdot}10^{21}\right) \tag{10}$$

$$\dot{S}_0 = 0.185\cdot\frac{\tanh\left(\frac{T-698}{50}\right)-\tanh\left(\frac{T-713}{50}\right)}{2\tanh\left(\frac{713-698}{100}\right)}\cdot\frac{1}{5{\cdot}10^{21}}$$

$$\Phi_0 = 60\cdot\frac{\tanh\left(\frac{T-623}{50}\right)-\tanh\left(\frac{T-793}{50}\right)}{2\tanh\left(\frac{793-623}{100}\right)}\cdot\left(5{\cdot}10^{21}\right) \tag{11}$$

where T (K) is the temperature. In Fig. 6, both the Lemehov et al. correlations (Eqs. 9–11) are plotted and compared to the two models already embedded in TRANSURANUS. The left plot (a) shows the predicted swelling behaviour as a function of the fast neutron fluence, at a temperature representative of MYRRHA cladding in normal operating conditions (i.e., 375°C), while the right plot (b) shows the strong dependence on temperature, at a neutron fluence typical of MYRRHA end-of-life conditions (10^{23} cm^{-2}). The comparison reveals a reduced swelling behaviour of DIN 1.4970 with respect to AIM1, especially in the temperature range 400°C – 550°C and high neutron fluence. Furthermore, it is expected that swelling will substantially affect the performance of the MYRRHA cladding, the maximum of the swelling curve being located in its operative temperature range (Fig. 6b).

4. Simulation results

Two simulation cases for the thermal–mechanical performance of the MYRRHA hottest pin under normal operating conditions have been considered. Firstly, a *reference case* has been analysed by employing the models recommended in TRANSURANUS for the MYRRHA operating conditions and pin materials. This scenario is intended to provide reference predictions of the MYRRHA hottest pin response. Secondly, a sensitivity analysis on a selected subset of TRANSURANUS models has been carried out involving the novel correlations presented in Section 3. This analysis has the objective of identifying *worst cases*, i.e., combinations of input models (still suitable for the MYRRHA pin materials and irradiation conditions) leading to the most severe pin performance according to some figures of merit (peak fuel and cladding temperatures, peak cladding stress and plastic strain). The *worst cases* are exploited to conservatively verify the compliance with the operative design limits (Table 2), even in the case of the most critical MYRRHA pin performance predicted by TRANSURANUS.

4.1. Simulation set-up

The TRANSURANUS code solves the fuel pin performance problem by discretizing the domain through a number of axial and radial nodes (1.5D spatial modelling) (European Commission, 2020). In this work, the computational mesh adopts 16 axial slices of equal length (4 cm each) and a total of 40 radial nodes denser towards the gap, as a result of a grid independence analysis on the MYRRHA fuel pin geometry. The mesh nodes are placed in the middle of the axial slices, as shown in Fig. 7, and the main pin geometry specifications are collected in Table 3.

For what concerns the MYRRHA *reference case* simulation, properties and phenomena involving the fuel, cladding and coolant are generally modelled employing the correlations recommended in TRANSURANUS (European Commission, 2020). The coolant (LBE) properties, e.g., thermal conductivity and dynamic viscosity, are modelled according to the OECD/NEA Handbook (OECD/NEA, 2007), while models suitable for the MYRRHA MOX fuel are adopted, including fuel densification (Dienst et al., 1979; Olander, 1976), relocation ((Preusser and Lassmann, 1983), calibrated on liquid–metal fast reactor conditions), grain growth (Ainscough et al., 1973; Botazzoli, 2011; Botazzoli et al., 2010), plutonium and americium redistribution (Di Marcello et al., 2014). The fuel restructuring model considers the pore movement for columnar grains and normal grain growth for equiaxed grains (limiting the grain size at 50 μm), while the fission gas diffusion equation is solved via the URGAS algorithm (Elton and Lassmann, 1987), with the diffusion coefficient by Matzke (Matzke, 1980) including a constant a-thermal component (European Commission, 2020). Fission gas release in the

[4] The damage dose dependence reported in the original paper (Lemehov et al., 2011) has been modified in a fluence dependence by adopting a conversion factor equal to $5{\cdot}10^{21}\,dpa^{-1}cm^{-2}$, appearing in Eqs. (10) and (11) and directly suggested by (Lemehov et al., 2011).

[5] In the original paper (Lemehov et al., 2011), there is a minus sign in front of the fraction at both the exponential arguments of Eq. (9). The present authors deem the minus as a typo, since the original correlation is incoherent with its own plot in the original paper (i.e., Fig. 3 in Ref. (Lemehov et al., 2011). For this reason, in this work the sign of the exponential arguments has been changed.

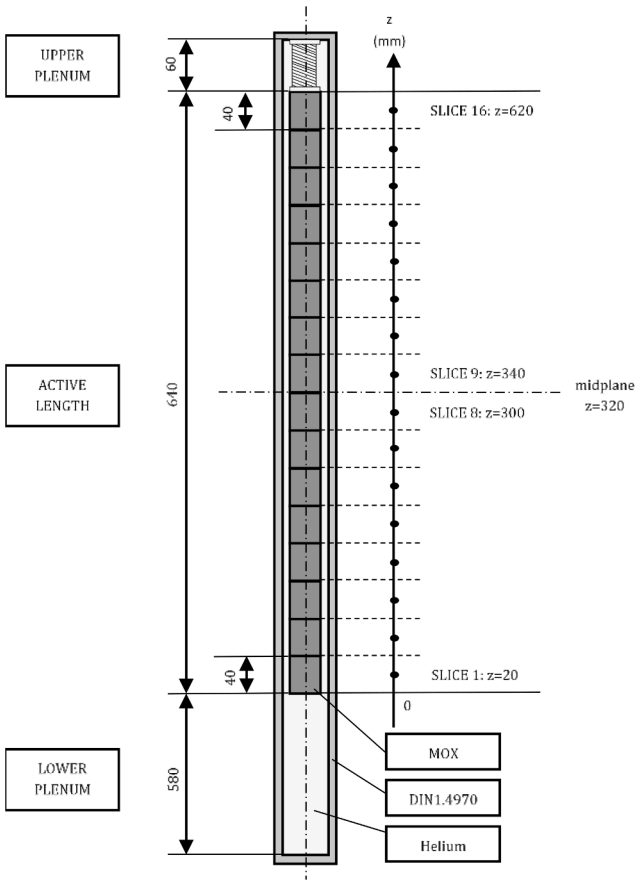

Fig. 7. MYRRHA fuel pin sketch (not to scale) and discretization in axial slices. The following figures (simulation results) refer to slice 9 and slice 16, at 340 mm and 620 mm from the bottom of fuel column, respectively.

Table 3
Geometry specifications of the as-fabricated MYRRHA fuel pin (Luzzi et al., 2019).

Geometry specifications	Value
Fuel outer diameter	5.42 mm
Cladding inner diameter	5.65 mm
Cladding outer diameter	6.55 mm
Active fuel length	650 mm
Upper plenum length	60 mm
Lower plenum length	580 mm

fuel-cladding gap is triggered by a saturation threshold for the coverage of grain boundaries by inter-granular fission gas bubbles (Pastore, 2012; Pastore et al., 2013). As for the cladding phenomena, the Többe creep correlations originally embedded in the code have been chosen for the *reference case* simulation (Eqs. (2) and (4), (Többe, 1975)), except for the CDF computation, for which the new (best-estimate) approach based on the LMP has been preferred (Eqs. 6–8). The aim of the reference simulation is indeed to provide the MYRRHA pin performance results from the basic v1m1j20 version of the TRANSURANUS code, provided that the standard TRANSURANUS models are suitable for 15-15Ti steels or for the specific MYRRHA cladding material (DIN 1.4970). The choice of the thermal creep correlation proves irrelevant at the low operative temperatures of the MYRRHA cladding (270–450°C), while creep is dominated by the irradiation component. The specific correlations for the void swelling of different versions of the DIN 1.4970 published by (Lemehov et al., 2011) are already considered for the reference simulation, employing the "B" correlation (Eqs. 9–10) being referred to a standard DIN 1.4970 steel prototypic for MYRRHA. The novel models presented in Section 3 of this paper have all been considered in the framework of sensitivity analyses devoted to the identification of *worst cases* for the MYRRHA hottest pin performance (Section 4.3).

4.2. Reference-case results

The fuel and cladding temperature evolutions during irradiation, at their respective axial hottest spots, are shown in Fig. 8. The cladding temperature follows the coolant one (Fig. 8a), in turn determined by the linear power and by the flow rate cooling the hottest pin during each batch. The cladding maximum temperature is reached at beginning of life (batch 1), at the uppermost slice of the fuel pin, and it approaches 450°C, while it falls to around 330°C at the end of life. Hence, a considerable margin with respect to the design limit on the peak cladding temperature, set to prevent fuel-side corrosion issues on the cladding inner surface (Table 2), is preserved throughout the irradiation history.

As for the fuel, the maximum temperature approaches 1700°C, satisfying with a large margin the conservative limit for fuel melting established for the MYRRHA fuel (Table 2). This value occurs near the pin mid-plane, at an axial elevation of 340 mm (slice 9, at the peak linear heat rate of 230 W cm^{-1}) and at the end of the first irradiation cycle (Fig. 8b). The fuel inner temperature reached at the end of the second irradiation cycle is similar, but slightly lower. The fuel temperature evolution is dominated by the fuel-cladding gap conductance, as shown in Fig. 9. The initial gap conductance drop is attributed to the high fission gas release (FGR) rate occurring until batch 2 (up to almost 30%), an effect prevailing over the simultaneous gap width reduction (Fig. 10). The fuel temperature decreases to 1130°C just before the final shutdown, following the progressive reduction of the MYRRHA linear heat rate along the irradiation batches (Fig. 2a) and the increase of the gap conductance due to the progressive reduction of the gap width.

The fuel temperatures predicted by TRANSURANUS are relatively low, preventing fuel restructuring whose onset is set to 1800°C, consistently with experimental observations (Lemehov et al., 2012; Gallais-During et al., 2018). Hence, the formation of columnar grains and of an inner void does not occur in the MYRRHA fuel according to the reference simulation, even in the hottest pin.

As far as cladding stresses and strains are concerned, the predicted values never exceed the elastic limit and keep well below the adopted design limit on the equivalent cladding stress (reported in Table 2 and recalled in Table 4). This design limit is provided in terms of the offset yield stress, i.e., the stress at which 0.2% plastic deformation of the material occurs ($\sigma_{0.2}$). Considering that the yield stress decreases with increasing temperature and that the cold-working process enhances the steel mechanical properties, a minimum value of 450 MPa for $\sigma_{0.2}$ can be conservatively adopted for the MYRRHA cladding at the highest operative temperature reached (450°C, Fig. 8a), coherently with what reported by (Holmstrom et al., 2017) for 24% cold-worked DIN 1.4970 and by (Strafella et al., 2017a,b) for 15-15Ti steels 20% cold-worked at 550°C. The adopted conservative value should also account for the irradiation effect on the yield stress of DIN 1.4970 cladding steels, for which suitable references have not been found in the current open literature (but the yield stress of other cladding steels slightly improves under fast neutron fluence, e.g., (Nakatsuka, 1991; Weir et al., 1968)). The peak equivalent cladding stress of 71 MPa resulting from the reference simulation (Table 4) is hence well below the adopted design limit ($2/3\ \sigma_{0.2} = 300$ MPa).

Since the cladding remains in the elastic deformation regime throughout the entire MYRRHA base irradiation history, the plastic strain remains null up to the end of life, also due to the absence, along the whole pin length, of gap closure and fuel-cladding mechanical interaction. As shown for the peak power node in Fig. 10, the differential thermal expansion between cladding and fuel pellet and the progressive fuel swelling (~ 3% at shutdown) cause the gap width reduction, reaching a minimum of 10.5 μm gap width at the end of irradiation

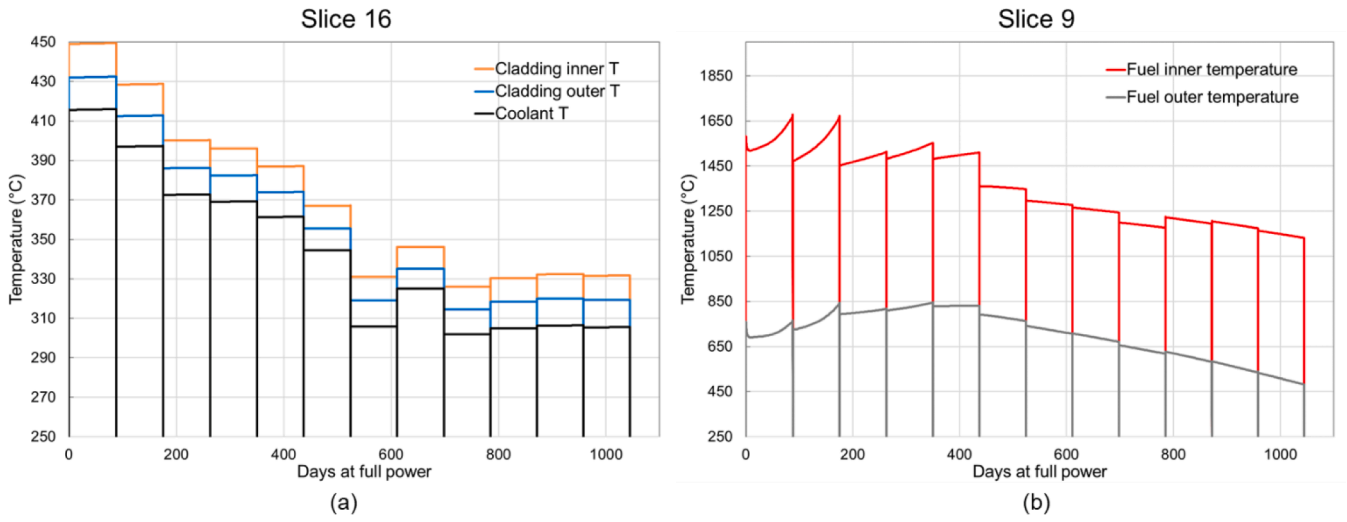

Fig. 8. Temperature evolutions during irradiation in (a) cladding, coolant and (b) fuel, referring to the respective hottest axial locations, as predicted by the MYRRHA *reference case* simulation.

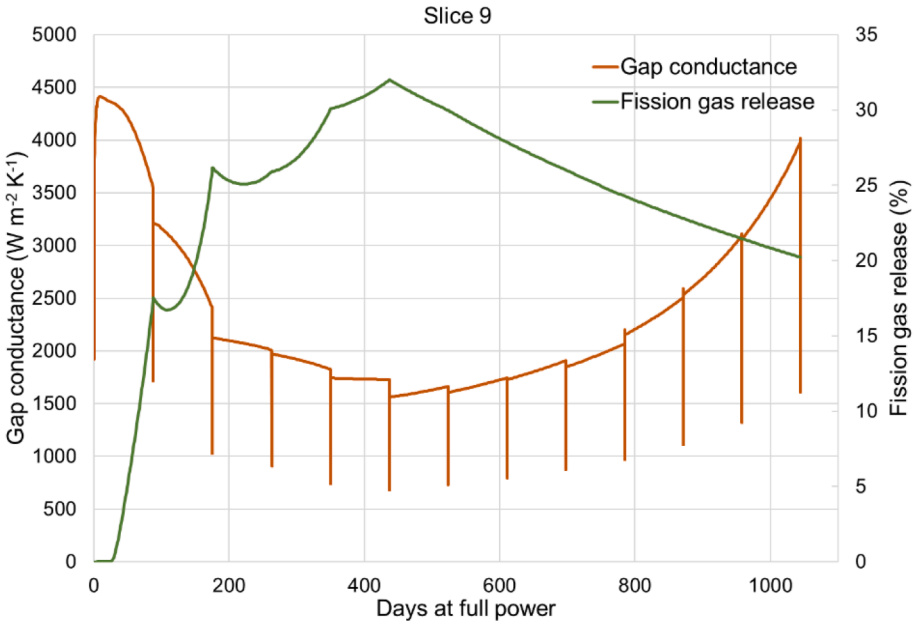

Fig. 9. Fuel-cladding gap conductance and fission gas release evolution during irradiation, at the axial peak power node, as predicted by the MYRRHA *reference case* simulation.

(batch 12, just before shutdown). In absence of PCMI, a contact pressure never develops, and the main sources of cladding stress are thermal gradients (limited, i.e., the maximum temperature gradient across the cladding is ~ 20°C, as shown in Fig. 8a) and mechanical loading of the cladding due to the gap and coolant (net) pressures acting on it. Accordingly, the radial average of the cladding equivalent stress reaches 34 MPa at most, insufficient to trigger an effective creep mechanism (especially considering the low cladding temperatures). The absence of significant cladding thermal creep strain and of cladding plasticity justifies the constant zero value of the CDF.

In Table 4, the maximum predicted values of the quantities to be monitored for the assessment of the MYRRHA hottest pin performance are summarized. The outcome is a complete compliance with the design limits assumed in this work. In fact, the cladding plastic strain and CDF limits are surely respected, the calculated values being null. The design limits on the cladding equivalent stress and on the peak fuel temperature are also respected with wide margins, far from cladding plasticity and fuel melting issues. The lowest margin holds for the cladding inner surface temperature, as its maximum value is 50°C below the corresponding limit. Nevertheless, fuel-side corrosion issues on the cladding inner surface are prevented given the compliance with the design limit.

It should be pointed out that the limits on the cladding plastic strain and on the CDF are provided for completeness. They become relevant for transient conditions, while even in the *worst cases* of MYRRHA normal operation considered in this study the maximum calculated values remain null (Section 4.3).

4.3. *Worst-case results*

The *worst cases* (WCs) for the MYRRHA case study have been identified by means of a multivariate sensitivity analysis, i.e., TRANSURANUS code simulations have been performed with every possible combination of selected models (Table 5), looking for the most severe scenarios in terms of different figures of merit. This methodology allows

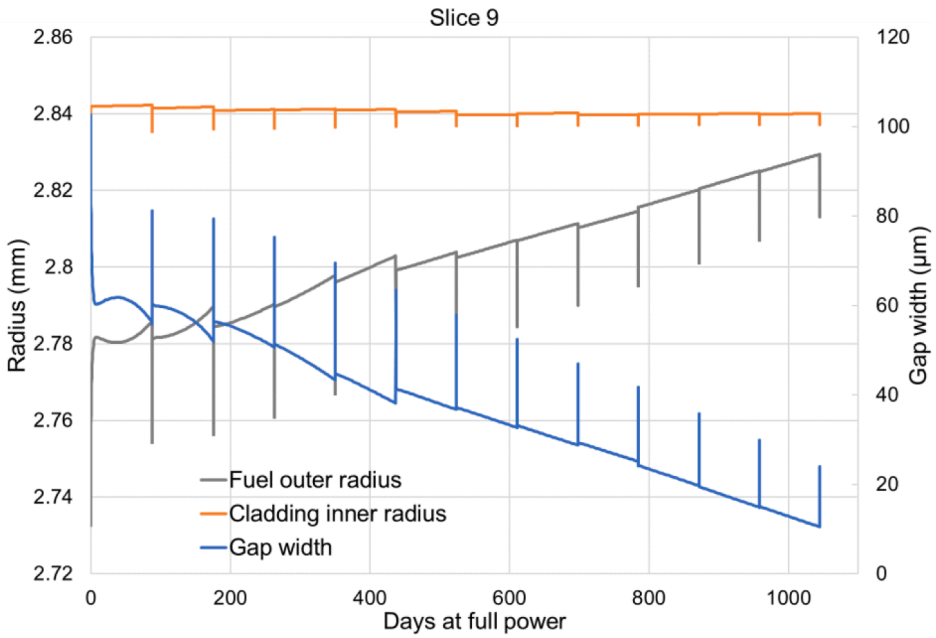

Fig. 10. Cladding inner radius, fuel outer radius and gap width evolution during irradiation, at the axial peak power node, as predicted by the MYRRHA *reference case* simulation.

Table 4
Maximum calculated temperatures, cladding equivalent strain and stress during irradiation, as predicted by the MYRRHA *reference case* simulation. The design limits assumed in the present work (Table 2) are here recalled for a direct comparison.

Quantity	Maximum value	Adopted design limit	Location (Fig. 7)
Peak fuel temperature	1680°C	2870 K (2597°C)	slice 9, end batch 1
Peak cladding inner surface temperature	449.4°C	500°C	slice 16, end batch 1
Peak cladding equivalent stress	71 MPa	$\frac{2}{3}\sigma_{0.2} = 300$ MPa	slice 7, end of batch 1, at cladding inner radius
Cladding equivalent plastic strain	0.00%	0.5%	–
Cladding CDF	0.00	1	–

to assess the selection of different material property models and their parameters, which is the major source of uncertainty in fuel performance calculations (Pastore et al., 2015; Bouloré, 2019), and their impact on the main pin performance outcomes. In the present work, the peak fuel temperature and the cladding permanent strain have been chosen as figures of merit, since both are subjected to relevant design limits (Table 2) and are among the main quantities of engineering interest for the pin safe operation. Fuel and cladding phenomena and properties, deemed relevant for the fuel temperature and cladding strain and affected by significant modelling uncertainties, have been involved in the analysis (considering models suitable for the MYRRHA pin materials and irradiation conditions). In particular, the fuel thermal conductivity has been selected as a major contributor to the peak fuel temperature, while the two cladding phenomena investigated in Section 3 (i.e., creep and void swelling) have been chosen related to the cladding strain. Fuel swelling has been included as well, being crucial for the gap

Table 5
Model options considered for the sensitivity analyses on the MYRRHA case study.

Phenomenon/ Property	*Reference case* model	Alternative options
Cladding thermal creep	Többe correlation (Többe, 1975)	Novel correlation - Thermal creep strain rate [a]
Cladding irradiation creep	Többe correlation (Többe, 1975)	Novel correlation - Irradiation creep strain rate [a]
Cladding void swelling	Lemehov et al. - B correlation (Lemehov et al., 2011) [a]	Lemehov et al. - L correlation (Lemehov et al., 2011) [a]
Fuel thermal conductivity	Van Uffelen et al. correlation (Schubert et al., 2004)	Van Uffelen et al. conservative correlation (Schubert et al., 2004) Carbajo et al. correlation (Carbajo et al., 2001) Philipponneau correlation (Philipponneau, 1992) Magni et al. correlation (Magni et al., 2020)
Fuel swelling	Preusser and Lassmann correlation (Preusser and Lassmann, 1983)	Pesl et al. correlation (Pesl et al., 1987)

[a] Novel correlation developed/implemented in the present work, in the framework of the TRANSURANUS code extension (Section 3).

dynamics and thus for exploring eventual scenarios characterized by gap closure[6], besides the impact of the gap conductance on the fuel temperature regime. The analysis involved both models and correlations already available in the TRANSURANUS code (adopted for the *reference case* simulation) and originally developed/implemented in this work (Section 3).

The model options considered in the analysis are summarized in Table 5. In Table 6, the correlation sets characterizing the *worst cases* for the two figures of merit, recognized among the 48 performance

[6] The fuel and cladding phenomena and properties not included in the sensitivity analysis have been modelled with the same options adopted for the *reference case* simulation (Section 4.1).

Table 6
Models leading to the *worst cases* (WCs) for the MYRRHA case study.

Phenomenon/ Property	WC - Peak fuel temperature	WC - Cladding permanent strain
Cladding thermal creep	Not relevant	Not relevant
Cladding irradiation creep	Novel correlation - Irradiation creep strain rate [a]	Novel correlation - Irradiation creep strain rate [a]
Cladding void swelling	Lemehov et al. - B correlation (Lemehov et al., 2011) [a]	Lemehov et al. - B correlation (Lemehov et al., 2011) [a]
Fuel thermal conductivity	Carbajo et al. correlation (Carbajo et al., 2001)	Van Uffelen et al. conservative correlation (Schubert et al., 2004)
Fuel swelling	Preusser and Lassmann correlation (Preusser and Lassmann, 1983)	Pesl et al. correlation (Pesl et al., 1987)

[a] Novel correlation developed/implemented in the present work, in the framework of the TRANSURANUS code extension (Section 3).

scenarios originating from the multivariate scheme[7], are reported. The sets of models leading to the *worst cases* for the MYRRHA hottest pin, in terms of fuel peak temperature or cladding permanent strain, are different, as emerges from Table 6. The cladding thermal creep model does not impact on the identification of the *worst cases*, since the thermal creep strain remains always null as in the *reference case* (due to the low temperatures of the MYRRHA cladding in normal operating conditions).

The resulting fuel inner and outer temperature trends for the *WC - Peak fuel temperature* are compared in Fig. 11 with the *reference case* results, at the hottest axial location. A discrepancy of around 100°C between the two scenarios is reached during the first two irradiation batches, while an almost constant increase of the fuel outer temperature (~ 50°C maximum) spreads throughout the entire irradiation history. The maximum peak fuel temperature approaches 1800°C in the *worst case*, localized at the end of batch 2. These temperature differences originate from the set of TRANSURANUS models associated to this *worst case*, ensuring the widest possible gap opening (i.e., the minimum gap conductance) and the lowest fuel thermal conductivity, provided by the Carbajo et al. correlation (Carbajo et al., 2001) (Table 6).

The model options producing the fastest cladding deformation mechanisms feature the *WC - Cladding permanent strain*. In particular, the *worst case* correlation adopted for the irradiation creep (i.e., the one developed in Section 3) causes the cladding creep strain to increase by one order of magnitude, while the cladding swelling correlation adopted in the *reference case* already provides the highest swelling rates (Fig. 6) and is hence kept in the *worst case*. Instead, the Pesl et al. correlation (Pesl et al., 1987) for fuel swelling (predicting a higher pellet swelling than the reference one (Preusser and Lassmann, 1983), i.e., slightly more than 4% at the final shutdown – end of batch 12) leads to gap closure at the beginning of batch 9, allowing PCMI to take place, as shown in Fig. 12 for the axial peak power node. Nevertheless, the developed contact pressure between pellet and cladding causes a maximum radial average of the cladding equivalent stress around 35 MPa, far below the yielding point and the corresponding design limit, and thus from inducing a plastic strain. Stress relaxation by irradiation creep, when the fuel-cladding contact is achieved, contributes to keep the cladding stress levels low also in PCMI conditions. Consequently, the cladding plastic strain remains null in the analysed *worst case* in terms of gap closure, as in the *reference case*.

In Table 7, the main outcomes from the simulation of the MYRRHA *worst case* in terms of peak fuel temperature are summarized. The maximum cladding temperature exhibits only a slight variation with respect to the *reference case* (Table 4), while the peak fuel temperature increases by ~ 100°C, still preserving a large safety margin to fuel melting. Also, the design limit on the cladding equivalent stress is respected with a large margin, the overall peak value being slightly lower than in the *reference case*. For what concerns the *worst case* in terms of cladding permanent strain, the conclusions are the same of the *reference case*, since the cladding equivalent plastic strain and the cladding CDF are still both null, hence fulfilling the corresponding design limits.

5. Conclusions

In this paper, the preliminary assessment of the thermal–mechanical behaviour of the MYRRHA fuel pin in normal operating conditions has been presented. The analysis has been performed by applying the TRANSURANUS fuel performance code (version v1m1j20), extended to allow the proper modelling of the creep and swelling responses of the specific cladding material adopted in the current MYRRHA pin design, i.e., the double stabilized 15-15Ti austenitic stainless steel DIN 1.4970. Based on a literature review and best fits of dedicated experimental data, novel correlations for the creep and void swelling behaviour of DIN 1.4970 have been developed and implemented in TRANSURANUS. Specifically, the proposed novel correlation for the irradiation creep strain rate allows more conservative estimations with respect to the state-of-the-art correlation of the TRANSURANUS code, at the fast neutron fluxes and equivalent stresses representative of the MYRRHA cladding in normal operating conditions, besides best-fitting the specific recent data for the DIN 1.4970 steel. Instead, thermal creep proves negligible at the low nominal temperatures of the MYRRHA cladding, although the original correlation herein developed allows more conservative estimations in the MYRRHA cladding temperature range. Moreover, the code has been equipped with dedicated correlations from literature describing the void swelling of DIN 1.4970 under irradiation.

The analysis of the MYRRHA fuel and cladding performance under irradiation focused on a *hypothetical* hottest pin, defined as located in the hottest positions during every irradiation batch and assumed to provide conservative predictions about the MYRRHA fuel pin behaviour. The *reference case* simulation consisted in employing the set of models for fuel and cladding phenomena and properties recommended by the state-of-the-art TRANSURANUS code, suitable for the MYRRHA pin materials and irradiation conditions. The comparison of the performance results with the corresponding design limits herein adopted for the MYRRHA case study showed complete compliance with the safety requirements in terms of cladding deformations and of fuel and cladding temperatures.

In addition to the reference calculations, a sensitivity analysis on selected models (cladding thermal and irradiation creep, fuel and cladding swelling, fuel thermal conductivity) has been performed, with the aim of identifying two different *worst-case* scenarios characterized by the worst pin response in terms of fuel temperature or cladding deformation, respectively. The high level of safety during the base irradiation of the MYRRHA hottest fuel pin is confirmed also in the obtained *worst cases*. The pin performance slightly worsens, showing fuel-cladding mechanical interaction leading to a weak contact pressure and a peak fuel temperature slightly higher than in the *reference case*. Nevertheless, the simulation results of the *worst-case* scenarios still yields large margins to the adopted design limits, since the peak fuel temperature remains much lower than the melting temperature of the MYRRHA irradiated MOX fuel and no cladding plastic strain still occurs.

The modelling advancements achieved in this work extend the capabilities of the TRANSURANUS fuel performance code of accurately simulating fast reactor and Generation IV fuel pins employing austenitic stainless-steel cladding materials. The herein adopted strategy led to the conservative assessment of the MYRRHA fuel pin performance in normal operating conditions, demonstrating at the same time the effectiveness of the TRANSURANUS code in providing safety indications about fuel

[7] The 48 scenarios correspond to the outcome from all the possible different combinations of the models reported in Table 5 for the selected fuel and cladding properties (cladding thermal and irradiation creep, fuel and cladding swelling, fuel thermal conductivity).

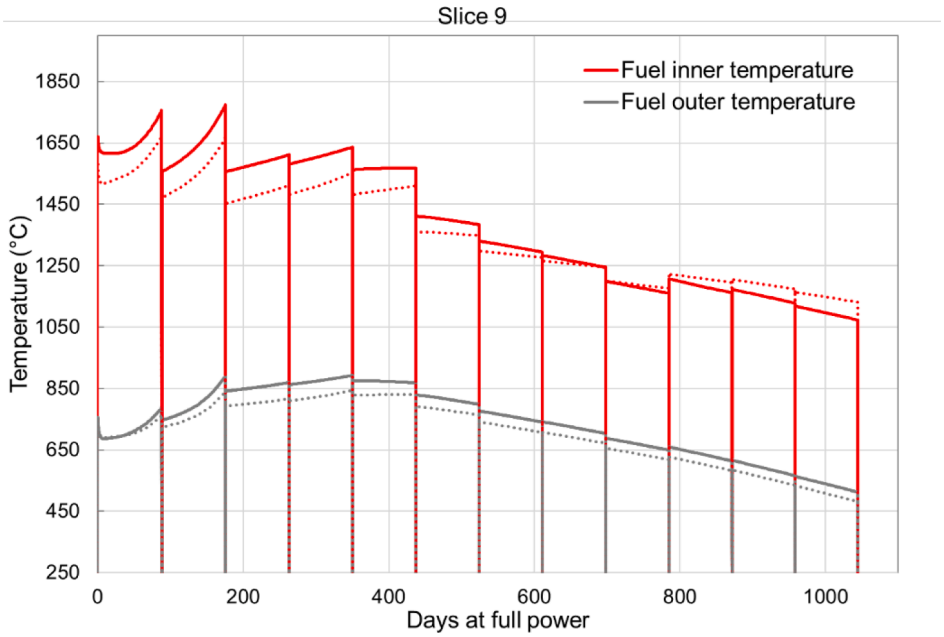

Fig. 11. Comparison between the evolution during irradiation of fuel inner and outer temperatures, at the axial peak power node, in the *reference case* (dotted lines) and in the *worst case* in terms of peak fuel temperature (solid lines).

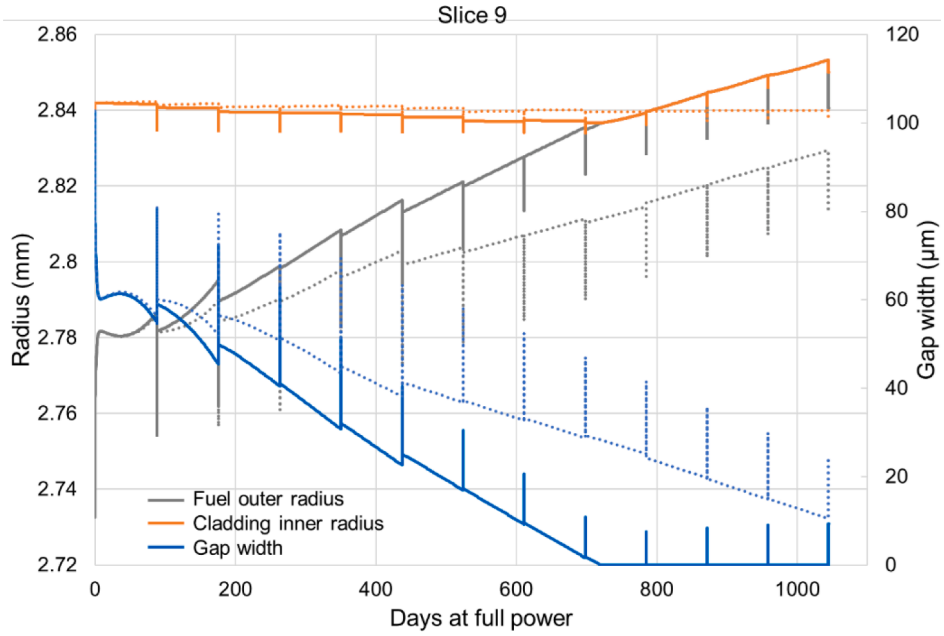

Fig. 12. Comparison between the evolution during irradiation of fuel outer radius, cladding inner radius and gap width at the axial peak power node, in the *reference case* (dotted lines) and in the *worst case* in terms of cladding permanent strain (solid lines).

Table 7
Maximum temperatures and equivalent cladding strain as predicted by the simulation of the MYRRHA *worst case* in terms of peak fuel temperature.

Quantity	Maximum value	Location
Peak fuel temperature	1774°C	slice 9, end batch 2
Peak cladding inner surface temperature	449.5°C	slice 16, end batch 1
Peak cladding equivalent stress	68 MPa	slice 10, beginning of batch 2, at cladding inner radius

pins designed for an ADS-LBE Generation IV fast reactor. This work can be considered as a starting point for further improvements and applications, either concerning the MYRRHA facility or other Generation IV reactor concepts. For example, a potential future development of this work, of sure interest in the framework of the design optimization of the MYRRHA reactor, would be accounting for the corrosion of the DIN 1.4970 cladding steel in liquid–metal environments, being a critical issue for the cladding performance but poorly considered up to now in fuel performance codes. To this end, additional experimental data currently missing (concerning also cladding creep in the specific MYRRHA irradiation conditions) would significantly support and improve the modelling activity. Moreover, the built-in Monte Carlo capabilities

of the TRANSURANUS code could be exploited to extend the performed sensitivity studies with an uncertainty analysis. Finally, the performance assessment of the MYRRHA fuel pins during operational transients (normal or off-normal) and accidental transients (such as design basis accidents), which was out of the scope of this paper, will be the object of future works.

CRediT authorship contribution statement

A. Magni: Investigation, Methodology, Software, Validation, Visualization, Writing – original draft, Writing – review & editing. **T. Barani:** Methodology, Software, Visualization, Writing – review & editing. **F. Belloni:** Data curation, Writing – review & editing. **B. Boer:** Conceptualization, Data curation, Writing – review & editing. **E. Guizzardi:** Investigation, Software, Validation, Visualization, Writing – review & editing. **D. Pizzocri:** Conceptualization, Investigation, Methodology, Software, Supervision, Validation, Visualization, Writing – review & editing. **A. Schubert:** Software, Writing – review & editing. **P. Van Uffelen:** Methodology, Software, Supervision, Visualization, Writing – review & editing. **L. Luzzi:** Funding acquisition, Project administration, Supervision, Visualization, Writing – review & editing.

Declaration of Competing Interest

The authors declare that they have no known competing financial interests or personal relationships that could have appeared to influence the work reported in this paper.

Acknowledgments

This work has received funding from the Euratom research and training programme 2014-2018 through the INSPYRE project under grant agreement No 754329.

References

Aït Abderrahim, H. Sobolev, V. Malambu, E. 2005. "Fuel design for the experimental ADS MYRRHA", in: *Technical Meeting on use of LEU in ADS,* 10-12 October 2005, IAEA, Vienna, Austria, pp. 1–13.

Agosti, F. Botazzoli, P. Di Marcello, V. Pastore, G. Luzzi, L. 2013. "Extension of the TRANSURANUS code to the analysis of cladding materials for liquid metal cooled fast reactors: A preliminary approach", Technical Report, Politecnico di Milano.

Agosti, F. Botazzoli, P. Di Marcello, V. Luzzi, L. Pastore, G. 2011. "Fuel rod performance analysis for the Italian LBE-XADS: a comparison of two different cladding materials", in: *Workshop on Technology and Components of Accelerator-driven Systems*, 15-17 March 2010, Karlsruhe, Germany.

Ainscough, J.B., Oldfield, B.W., Ware, J.O., 1973. Isothermal grain growth kinetics in sintered UO_2 pellets. J. Nucl. Mater. 49 (2), 117–128.

Aït Abderrahim, H., Baeten, P., De Bruyn, D., Fernandez, R., 2012. MYRRHA - A multi-purpose fast spectrum research reactor. Energy Convers. Manag. 63, 4–10.

Aït Abderrahim, H., Baeten, P., Sneyers, A., Schyns, M., Schuurmans, P., Kochetkov, A., Van den Eynde, G., Biarrotte, J.-L., Garbil, R., Davies, C., Diaconu, D., 2020. Partitioning and transmutation contribution of MYRRHA to an EU strategy for HLW management and main achievements of MYRRHA related FP7 and H2020 projects: MYRTE, MARISA, MAXSIMA, SEARCH, MAX, FREYA, ARCAS. Nucl. Sci. Technol. 6, 33. https://doi.org/10.1051/epjn/2019038.

Aitken, E. A. Evans, S. K. 1968. "A thermodynamic data program involving plutonia and urania at high temperatures", Report GEAP-5720.

Aït Abderrahim, H., De Bruyn, D., Dierckx, M., Fernandez, R., Popescu, L., Schyns, M., Stankovskiy, A., Van Den Eynde, G., Vandeplassche, D., 2019. MYRRHA accelerator driven system programme: Recent progress and perspectives. Nucl. Power Eng. 2, 29–41.

Beck, T., Blanc, V., Escleine, J.-M., Haubensack, D., Pelletier, M., Phelip, M., Perrin, B., Venard, C., 2017. Conceptual design of ASTRID fuel sub-assemblies. Nucl. Eng. Des. 315, 51–60.

Boer, B., Lemehov, S., Sobolev, V., Verwerft, M., 2012. Fuel performance assessment of the lead-bismuth cooled MYRRHA reactor. Trans. Am. Nucl. Soc. 1201–1204.

Botazzoli, P. 2011. "Helium production and behaviour in LWR nuclear oxide fuels", PhD thesis, Politecnico di Milano, Italy.

Botazzoli, P. Luzzi, L. Bremier, S. Schubert, A. Van Uffelen, P. 2010. "Microstructural Evolution in Heterogeneous and Homogeneous MOX Fuels", in: *NuMat - The Nuclear Materials Conference 2010,* 4-7 October 2010, Karlsruhe, Germany.

Bouineau, V. Di Marcello, V. Lainet, M. Van Uffelen, P. Walker, C. T. Chauvin, N. Pelletier, M. 2013. "Assessment of SFR fuel pin performance codes under advanced fuel for minor actinide transmutation", in: *Proceedings of the International Nuclear Fuel Cycle Conference GLOBAL 2013*, September 29–October 3, 2013, Salt Lake City, USA.

Bouloré, A., 2019. Importance of uncertainty quantification in nuclear fuel behaviour modelling and simulation. Nucl. Eng. Design 355, 110311. https://doi.org/10.1016/j.nucengdes.2019.110311.

Bradbury, M.H., Pickering, S., Whitlow, W.H., 1978. A proposed mechanism for internal cladding corrosion in LMFBR mixed oxide fuel pins. J. Nucl. Mater. 78 (2), 272–280.

Carbajo, J.J., Yoder, G.L., Popov, S.G., Ivanov, V.K., 2001. A review of the thermophysical properties of MOX and UO_2 fuels. J. Nucl. Mater. 299 (3), 181–198.

Cautaerts, N., Delville, R., Dietz, W., Verwerft, M., 2017. Thermal creep properties of Ti-stabilized DIN 1.4970 (15–15Ti) austenitic stainless steel pressurized cladding tubes. J. Nucl. Mater. 493 (2017), 154–167.

Cechet, A., Altieri, S., Barani, T., Cognini, L., Lorenzi, S., Magni, A., Pizzocri, D., Luzzi, L., 2021. A new burn-up module for application in fuel performance calculations targeting the helium production rate in $(U, Pu)_O2$ for fast reactors. Nucl. Eng. Technol. 53, 1893–1908.

De Bruyn, D., Abderrahim, H.A., Baeten, P., Leysen, P., 2015. The MYRRHA ADS project in Belgium enters the Front End Engineering Phase. Phys. Procedia 66, 75–84.

De Bruyn, D. Fernandez, R. Engelen, J. 2016. "Recent Developments in the Design of the Belgian MYRRHA ADS Facility", in: *2016 International Congress on Advances in Nuclear Power Plants (ICAPP'16)*, San Francisco, California, USA, pp. 286–293.

Di Marcello, V., Schubert, A., van de Laar, J., Van Uffelen, P., 2012. Extension of the TRANSURANUS plutonium redistribution model for fast reactor performance analysis. Nucl. Eng. Des. 248, 149–155.

Di Marcello, V., Rondinella, V.V., Schubert, A., van de Laar, J., Van Uffelen, P., 2014. Modelling actinide redistribution in mixed oxide fuel for sodium fast reactors. Prog. Nucl. Eng. 72, 83–90.

Dienst, W. Muelle-Lyda, I. Zimmermann, H. 1979. "Swelling, densification and creep of oxide and carbide fuels under irradiation", in: *International conference on fast breeder reactor performance*, 5-8 March 1979, Monterey, California, USA, pp. 166–175.

EERA-JPNM, "INSPYRE - Investigations Supporting MOX Fuel Licensing in ESNII Prototype Reactors", 2017. [Online]. Available: http://www.eera-jpnm.eu/inspyre/.

Elton, P.T., Lassmann, K., 1987. Calculational methods for diffusional gas release. Nucl. Eng. Des. 101 (3), 259–265.

Engelen, J., Aït Abderrahim, H., Baeten, P., De Bruyn, D., Leysen, P., 2015. MYRRHA: Preliminary front-end engineering design. Int. J. Hydrogen Energy 40 (44), 15137–15147.

ESNII, "A contribution to the EU Low Carbon Energy Policy: Demonstration Programme for Fast Neutron Reactors", Concept Paper, pp. 1–6, 2010. Available: https://snetp.eu/wp-content/uploads/2020/06/ESNII-A-contribution-to-the-EU-Low-Carbon-Energy-Policy-May-2010.pdf.

European Commission, 2020. TRANSURANUS Handbook. Joint Research Centre, Karlsruhe, Germany.

Gallais-During, A., Delage, F., Béjaoui, S., Lemehov, S., Somers, J., Freis, D., Maschek, W., Van Til, S., D'Agata, E., Sabathier, C., 2018. Outcomes of the PELGRIMM project on Am-bearing fuel in pelletized and spherepac forms. J. Nucl. Mater. 512, 214–226.

GIF (Generation IV International Forum), "Technology Roadmap Update for Generation IV Nuclear Energy Systems", 2014. Available: https://www.gen-4.org/gif/upload/docs/application/pdf/2014-03/gif-tru2014.pdf.

Grasso, G., Petrovich, C., Mattioli, D., Artioli, C., Sciora, P., Gugiu, D., Bandini, G., Bubelis, E., Mikityuk, K., 2014. The core design of ALFRED, a demonstrator for the European lead-cooled reactors. Nucl. Eng. Des. 278, 287–301.

Grossbeck, M.L., Ehrlich, K., Wassilew, C., 1990. An assessment of tensile, irradiation creep, creep rupture, and fatigue behavior in austenitic stainless steels with emphasis on spectral effects. J. Nucl. Mater. 174 (2-3), 264–281.

Y. Guerin, "Fuel Performance of Fast Spectrum Oxide Fuel", in: *Comprehensive Nuclear Materials*, Vol. 2, Elsevier Inc., pp. 548-578, 2012.

Holmstrom, S., Simonovski, I., de Haan, F., Lapetite, J.-M., Baraldi, D., Serrano, M., Altstadt, E., Aktaa, J., Radu, V., Namburi, H., Cristalli, C., Pohja, R., Delville, R., Courcelle, A., 2017. "Determination of high temperature material properties of 15–15Ti steel by small specimen techniques", Report EUR 28746 EN. Publications Office of the European Union, Luxembourg.

Kato, M., Morimoto, K., Sugata, H., Konashi, K., Kashimura, M., Abe, T., 2008. Solidus and liquidus temperatures in the UO_2-PuO_2 system. J. Nucl. Mater. 373 (1-3), 237–245.

O. Klok, 2018. "Liquid Metal Corrosion Effects in MYRRHA candidate 316L Austenitic Stainless Steel", PhD thesis, Vrije Universiteit Brussel, Belgium.

Larson, F.R., Miller, J., 1952. Time-Temperature Relationship for Rupture and Creep Stresses. Trans. ASME 74, 765–771.

Lassmann, K., 1978. URANUS - A computer programme for the thermal and mechanical analysis of the fuel rods in a nuclear reactor. Nucl. Eng. Des. 45 (2), 325–342.

Lassmann, K., 1992. TRANSURANUS: a fuel rod analysis code ready for use. J. Nucl. Mater. 188, 295–302.

Lassmann, K., Moreno, A., 1977. The Light-Water-Reactor Version of the URANUS Integral Fuel-Rod Code. Atomkernenergie 30, 207–215.

Lemaignan, C. 2010. "Nuclear Materials and Irradiation Effects", in: *Handbook of Nuclear Engineering*, Springer, Ed., pp. 543–642, 2010.

Lemehov, S. Govers, K. Verwerft, M.2004. "Modelling non-standard mixed oxide fuels with the mechanistic code MACROS: Neutronic and heterogeneity effects", in: *Technical committee meeting on advanced fuel pellet materials and designs for water cooled reactors*, 20-24 October 2003, Brussels, Belgium, IAEA-TECDOC-1416, pp. 235-255.

Lemehov, S. Verwerft, M. Sobolev, V. 2005. "Thermomechanical modeling of prototypic targets containing high concentrations of minor actinides", in: *Fuels and Materials for Transmutation*, Technical Report NEA No. 5419, OECD/NEA.

Lemehov, S., Jutier, F., Parthoens, Y., Vos, B., Van Den Berghe, S., Verwerft, M., Nakae, N., 2012. MACROS benchmark calculations and analysis of fission gas release in MOX with high content of plutonium. Prog. Nucl. Energy 57, 117–124.

Lemehov, S., Sobolev, V.P., Verwerft, M., 2011. Predicting thermo-mechanical behaviour of high minor actinide content composite oxide fuel in a dedicated transmutation facility. J. Nucl. Mater. 416 (1–2), 179–191.

Luzzi, L., Cammi, A., Di Marcello, V., Lorenzi, S., Pizzocri, D., Van Uffelen, P., 2014. Application of the TRANSURANUS code for the fuel pin design process of the ALFRED reactor. Nucl. Eng. Des. 277, 173–187.

Luzzi, L. Barani, T. Magni, A. Pizzocri, D. Schubert, A. Van Uffelen, P. Marelle, V. Michel, B. Boer, B. Lemehov, S. Del Nevo, A. 2019. "Definition of detailed configurations of the case studies for the fuel performance simulations in Task 7.3", INSPYRE Milestone MS16, version 1.

Luzzi, L. Lorenzi, S. Pizzocri, D. Aly, A. Rozzia, D. Del Nevo, A. 2014. "Modeling and Analysis of Nuclear Fuel Pin Behavior for Innovative Lead Cooled FBR", Report RdS/PAR2013/022.

Lyon, W.L., Baily, W.E., 1967. The solid-liquid phase diagram for the UO2-PuO2 system. J. Nucl. Mater. 22 (3), 332–339.

Magni, A., Barani, T., Luzzi, L., Pizzocri, D., Schubert, A., Van Uffelen, P., Del Nevo, A., 2020. Modelling and assessment of thermal conductivity and melting behaviour of MOX fuel for fast reactor applications. J. Nucl. Mater. 541, 152410.

Magni, A., Luzzi, L., Pizzocri, D., Schubert, A., Van Uffelen, P., Del Nevo, A., 2021. Modelling of thermal conductivity and melting behaviour of minor actinide-MOX fuels and assessment against experimental and molecular dynamics data. J. Nucl. Mater. 557, 153312.

Matthews, J.R., Finnis, M.W., 1988. Irradiation creep models - an overview. J. Nucl. Mater. 159, 257–285.

Matzke, H.J., 1980. Gas release mechanisms in UO_2 - A critical review. Radiat. Eff. 53 (3-4), 219–242.

OECD/NEA, Handbook on Lead-bismuth Eutectic Alloy and Lead Properties, Materials Compatibility, Thermal-hydraulics and Technologies, Technical Report NEA No. 6195, OECD/NEA, 2007.

D. Olander, 1976. *Fundamental aspects of nuclear reactor fuel elements*, Technical Information Center, Office of Public Affairs, Energy Research and Development Administration.

Nakatsuka, Masafumi, 1991. Mechanical Properties of Neutron Irradiated Fuel Cladding Tubes. J. Nucl. Sci. Technol. 28 (4), 356–368.

Pastore, G., 2012. Modelling of Fission Gas Swelling and Release in Oxide Nuclear Fuel and Application to the TRANSURANUS Code. Politecnico di Milano, Italy. PhD thesis.

G. Pastore, P. Botazzoli, V. Di Marcello, and L. Luzzi, "Simulation of Power Ramp Tested LWR Fuel Rods by means of the TRANSURANUS Code", in: *Proceedings of Water Reactor Fuel Performance Meeting - WRFPM / Top Fuel 2009*, 6-10 September 2009, Paris, France, pp. 223–232, 2009.

Pastore, G., Luzzi, L., Di Marcello, V., Van Uffelen, P., 2013. Physics-based modelling of fission gas swelling and release in UO_2 applied to integral fuel rod analysis. Nucl. Eng. Des. 256, 75–86.

Pastore, Giovanni, Swiler, L.P., Hales, J.D., Novascone, S.R., Perez, D.M., Spencer, B.W., Luzzi, L., Van Uffelen, P., Williamson, R.L., 2015. Uncertainty and sensitivity analysis of fission gas behavior in engineering-scale fuel modeling. J. Nucl. Mater. 456, 398–408.

Pesl, R., Freund, D., Gärtner, H., Steine, H., 1987. "SATURN-S Ein Programmsystem zur Beschreibung des thermomechanischen Verhaltens von Kernreaktorbrennstäben unter Bestrahlung", *Technischer Bericht, KFK 4272*. Kernforschungszentrum Karlsruhe, Germany.

Philipponneau, Y., 1992. Thermal conductivity of (U, Pu)O_{2-x} mixed oxide fuel. J. Nucl. Mater. 188, 194–197.

Pioro, I.L., 2016. Handbook of Generation IV Nuclear Reactors. Elsevier Ltd., Woodhead Publishing.

Pitner, A.L., Gneiting, B.C., Bard, F.E., 1995. Irradiation performance of fast flux test facility drivers using D9 alloy. Nucl. Technol. 112 (2), 194–203.

Pizzocri, D., Barani, T., Luzzi, L., 2020. SCIANTIX: A new open source multi-scale code for fission gas behaviour modelling designed for nuclear fuel performance codes. J. Nucl. Mater. 532, 152042.

Pónya, P., Czifrus, S., 2017. Core optimisation issues of MOX fueled ALLEGRO reactor. Ann. Nucl. Energy 108, 188–197.

Preusser, T. Lassmann, K. 1993. "Current Status of the Transient Integral Fuel Element Performance Code URANUS", in: SMiRT 7, 22-26 August 1983, Chicago, USA.

Schroeder, H., 1986. In-beam creep rupture properties of DIN 1.4970 austenitic stainless steel at 873 K. J. Nucl. Mater. 141–143, 476–481.

Schubert, A. Van Uffelen, P. van de Laar, J. Sheindlin, M. Ott, L. 2004. "Present Status of the MOX Version of the TRANSURANUS Code", in: *Enlarged Halden Programme Group Meeting on High Burn-up Fuel Performance, Safety and Reliability*, 9-14 May 2004, Sandefjord, Norway.

Stainsby, R., Peers, K., Mitchell, C., Poette, C., Mikityuk, K., Somers, J., 2011. Gas cooled fast reactor research in Europe. Nucl. Eng. Des. 241, 3481–3489.

Strafella, A., Coglitore, A., Salernitano, E., 2017a. Creep behaviour of 15–15Ti(Si) austenitic steel in air and in liquid lead at 550°C. Procedia Struct. Integr. 3, 484–497.

Strafella, A., Coglitore, A., Fabbri, P., Salernitano, E., 2017b. 15-15Ti(Si) austenitic steel: creep behaviour in hostile environment. Frat. ed Integrità Strutt. 42, 352–365.

Többe, H., 1975. "Das Brennstabrechenprogramm IAMBUS zur Auslegung von Schellbrüter Brennstäben. Interatom - Technischer Bericht 75, 65.

Van Den Eynde, G., Malambu, E., Stankovskiy, A., Fernandez, R., Baeten, P., 2015. An updated core design for the multi-purpose irradiation facility MYRRHA. J. Nucl. Sci. Technol. 52 (7–8), 1053–1057.

Van Tichelen, K., Kennedy, G., Mirelli, F., Marino, A., Toti, A., Rozzia, D., Cascioli, E., Keijers, S., Planquart, P., 2020. Advanced Liquid-Metal Thermal-Hydraulic Research for MYRRHA. Nucl. Technol. 206 (2), 150–163.

Van Uffelen, P., Győri, C., Schubert, A., van de Laar, J., Hózer, Z., Spykman, G., 2008. Extending the application range of a fuel performance code from normal operating to design basis accident conditions. J. Nucl. Mater. 383 (1-2), 137–143.

P. Van Uffelen, M. Suzuki, "Oxide fuel performance modeling and simulations", in: *Comprehensive Nuclear Materials*, Vol. 3, Elsevier Inc., pp. 535–577, 2012.

Waltar, A. E. Todd, D. R. Tsvetkov, P. V. 2012. *Fast Spectrum Reactors*, Springer.

J. R. Weir, J. O. Stiegler, E. E. Bloom, 1968. "Irradiation behavior of cladding and structural materials", Report ORNL-TM-2258.

Yamamoto, K., Hirosawa, T., Yoshikawa, K., Morozumi, K., Nomura, S., 1993. Melting temperature and thermal conductivity of irradiated mixed oxide fuel. J. Nucl. Mater. 204, 85–92.

Yamamoto, N., Schroeder, H., 1988. In-beam creep rupture properties of cold-worked DIN 1.4970 and AISI 316 L at 873 K. J. Nucl. Mater. 155–157, 1043–1048.